

CONSERVATIVE SEMI-LAGRANGIAN SCHEMES FOR A GENERAL CONSISTENT BGK MODEL FOR INERT GAS MIXTURES

SEUNG YEON CHO, SEBASTIANO BOSCARINO, MARIA GROPPI, AND GIOVANNI RUSSO

ABSTRACT. In this work, we propose a class of high order semi-Lagrangian scheme for a general consistent BGK model for inert gas mixtures. The proposed scheme not only fulfills indifferiability principle, but also asymptotic preserving property, which allows us to capture the behaviors of hydrodynamic limit models. We consider two hydrodynamic closure which can be derived from the BGK model at leading order: classical Euler equations for number densities, global velocity and temperature, and a multi-velocities and temperatures Euler system. Numerical simulations are performed to demonstrate indifferiability principle and asymptotic preserving property of the proposed conservative semi-Lagrangian scheme to the Euler limits.

1. INTRODUCTION

Relaxation time approximations of BGK type for the Boltzmann equation are fundamental tools in order to properly describe several regimes of gas dynamics, where the macroscopic approach is not adequate. Indeed, the Boltzmann equation [10] is difficult to treat both from an analytical and a numerical point of view, due to its highly nonlinear integral collision operator, whereas BGK models [3, 29] retain the essential features of the Boltzmann equation with a simpler structure. The extension of BGK models to mixtures of gases is not trivial, since some drawbacks can arise, like loss of positivity of temperature and violation of the indifferiability principle. To our knowledge, the first mathematical approach to the construction of BGK models for mixtures was presented in [2], where the questions of consistency of the model and its generality were addressed. Generality means that the model is valid for any number of components of the mixture; consistency means exact conservation laws, fulfilment of the H-Theorem and uniqueness of equilibrium solutions. The model proposed in [2] was based on a single relaxation operator for each species, which reproduces the structure of the BGK operator for a single gas. Later, different BGK models have been introduced, having the same structure and allowing also to describe simple bimolecular chemical reactions in mixtures [19, 17] as well as polyatomic gases [6].

Recently, in [7] a general consistent BGK model for inert mixtures of monoatomic gases has been proposed, which mimics instead the structure of the Boltzmann equations for mixtures, with a collision operator for each species that is a sum of bi-species BGK operators.

In this paper we propose high order semi-Lagrangian schemes for this general BGK model for mixtures. Semi-Lagrangian schemes have been widely adopted for solving BGK type-models of the Boltzmann equation, since they do not require stability restriction on time step. In [26], authors first applied semi-Lagrangian method to the classical BGK equation for a single gas, combined with L-stable time discretization, which enables one to avoid the time step restrictions coming from the convective term and small relaxation time. This approach has been then adopted with linear multi-step methods such as backward difference formula (BDF) in [17] to design more efficient schemes. In [8], authors verify

that the schemes [17, 26] are not conservative and cannot exactly capture the behavior of Euler system when the Knudsen number ε tends to zero. This so called asymptotic preserving property (AP) can be attained indeed using conservative schemes, (see also [21]). To this aim, a predictor-corrector type semi-Lagrangian scheme is introduced in [8] to attain conservation up to machine precision. Although this AP scheme allows one to use large time step, it has severe time step restriction for large relaxation time. As a remedy of this, in [13] authors also modify the high order semi-Lagrangian methods [26, 17] by making use of a conservative reconstruction technique [12] for the interpolation together with the construction of conservative Maxwellian introduced in [24, 16]. This conservative scheme allows large time step for all ranges of relaxation time, and capture the correct behavior of Euler system in the limit $\varepsilon \rightarrow 0$. In the context of inert gas mixtures, a semi-Lagrangian approach has been already applied to BGK-type models in [18]. Although that method is designed to be high order without splitting based on [17], it is not conservative. In this paper, we focus on high order conservative semi-Lagrangian schemes with asymptotic property and we apply them to a general consistent BGK model for inert mixture [7], making use also of conservative reconstruction technique in [12].

The semi-Lagrangian approximation of the BGK equations is tested versus the Euler systems that can be obtained as a zero order level of any asymptotic expansion with respect to a proper Knudsen number. In this respect two hydrodynamic closures can be deduced from general consistent model [7], leading to classic Euler equations for number densities, global velocity and temperature or to multi-velocity and multi-temperature Euler system.

The paper is organized as follows. In section 2, we review the basic properties of the Boltzmann equations, the general BGK model for mixtures and their macroscopic Euler closures. Section 3 is devoted to the derivation of the first order semi-Lagrangian scheme for the general BGK model. In section 4, we extend it to high order semi-Lagrangian schemes. Then, in section 5 we present several numerical tests to verify the performance of the proposed schemes, with particular attention to the indifferentiability principle and AP property. Some concluding remarks end the paper.

2. KINETIC MODELS FOR INERT GAS MIXTURES

2.1. The Boltzmann equation for inert gas mixtures. Let us consider distribution functions $\{f_s(x, v, t), s = 1, \dots, L\}$ of L -species inert gases defined on phase space $(x, v) \in \mathbb{R}^3 \times \mathbb{R}^3$ at time $t > 0$. Under the assumption that s -th gas has a mass $m_s > 0$, the dynamics of a mixture of L inert rarefied gases can be described by the set of L Boltzmann-type equations:

$$(2.1) \quad \frac{\partial f_s}{\partial t} + v \cdot \nabla_x f_s = Q_s, \quad s = 1, \dots, L,$$

where the collision operator Q_s for s -species gas is given by

$$Q_s = \sum_{k=1}^L Q_{sk}(f_s, f_k).$$

The binary collision operator Q_{sk} is defined by

$$(2.2) \quad Q_{sk}(f_s, f_k) = \int_{\mathbb{R}^3 \times \mathbb{S}^2} dw d\omega g_{sk}(|y|, \hat{y} \cdot \omega) \left[f_s(v') f_k(w') - f_s(v) f_k(w) \right],$$

where g_{sk} is a nonnegative scattering kernel. In (2.2), we use an integration variable $w \in \mathbb{R}^3$, a unit vector on a sphere $\omega \in \mathbb{S}^2$, a relative velocity $y := v - w$ and its unit vector $\hat{y} := y/|y|$.

In the collision between s - and k -species gases, the pre-collisional velocities \mathbf{v} , \mathbf{w} and post collisional velocities \mathbf{v}' and \mathbf{w}' are related as follows:

$$\mathbf{v}' = \frac{m_s \mathbf{v} + m_k \mathbf{w}}{m_s + m_k} + \frac{m_k}{m_s + m_k} |y| \boldsymbol{\omega}, \quad \mathbf{w}' = \frac{m_s \mathbf{v} + m_k \mathbf{w}}{m_s + m_k} - \frac{m_s}{m_s + m_k} |y| \boldsymbol{\omega}.$$

We recall that the collision operator Q_s has the following properties:

- Conservation laws:

$$\langle Q_s, 1 \rangle = 0, \quad \sum_{s=1}^L m_s \langle Q_s, \mathbf{v} \rangle = 0, \quad \sum_{s=1}^L m_s \langle Q_s, |\mathbf{v}|^2 \rangle = 0$$

where

$$\langle f, h \rangle := \int_{\mathbb{R}^3} d\mathbf{v} f(\mathbf{v}) h(\mathbf{v}).$$

- H-theorem:

$$\sum_{s=1}^L \langle Q_s, \log f_s \rangle \leq 0$$

- Uniqueness of equilibrium:

$$Q_s = 0, \quad s = 1, \dots, L \quad \implies \quad f_s = n_s M(\mathbf{v}; u_s, \frac{K_B T_s}{m_s})$$

where

$$(2.3) \quad M = M(\mathbf{v}; a, b) \equiv \left(\frac{1}{2\pi b} \right)^{3/2} \exp \left(-\frac{1}{2b} |\mathbf{v} - a|^2 \right)$$

and K_B stands for the Boltzmann constant.

- Indifferentiability principle: this means that the sum of distribution function $f = \sum_{s=1}^L f_s$ obeys the single gas Boltzmann equation if all m_s and collision kernel g_{sk} are identical.
- Exchange rates of momentum and energy for each pair of species s and k :

$$\begin{aligned} \langle Q_{sk}, \mathbf{v} \rangle &= -\frac{m_k}{m_s + m_k} \langle \langle \mathbf{v} - \mathbf{w} \rangle \rangle_{sk} \\ \langle Q_{sk}, |\mathbf{v}|^2 \rangle &= -\frac{2m_k}{(m_s + m_k)^2} \langle \langle (m_s \mathbf{v} + m_k \mathbf{w}) \cdot (\mathbf{v} - \mathbf{w}) \rangle \rangle_{sk} \end{aligned}$$

where

$$\begin{aligned} \langle \langle \psi(\mathbf{v}, \mathbf{w}) \rangle \rangle_{sk} &= \int_{\mathbb{R}^3 \times \mathbb{R}^3} d\mathbf{v} d\mathbf{w} f_s(\mathbf{v}) f_k(\mathbf{w}) g_{sk}^{(1)}(|\mathbf{v} - \mathbf{w}|) \psi(\mathbf{v}, \mathbf{w}) \\ g_{sk}^{(1)}(|y|) &= 2\pi \int_{-1}^1 d\mu (1 - \mu) g_{sk}(|y|, \mu), \quad y \in \mathbb{R}^3. \end{aligned}$$

In this paper, we consider Maxwell molecules, for which the cross section g_{sk} is independent of $|y|$, i.e.,

$$(2.4) \quad g_{sk}^{(1)}(|y|) = \lambda_{sk} = \text{const},$$

Consequently,

$$(2.5) \quad \begin{aligned} \langle Q_{sk}, \mathbf{v} \rangle &= -\frac{m_k}{m_s + m_k} \lambda_{sk} n_s n_k (u_s - u_k) \\ \langle Q_{sk}, |\mathbf{v}|^2 \rangle &= -\frac{2m_k}{(m_s + m_k)^2} \lambda_{sk} n_s n_k [3(K_B T_s - K_B T_k) + (m_s u_s + m_k u_k) \cdot (u_s - u_k)] \end{aligned}$$

For the details of this calculation and other possible choices of g_{sk} , we refer to [7] and references therein.

- Macroscopic variables: for s -species gas, we define number density n_s , average velocity u_s , absolute temperature T_s by

$$(2.6) \quad n_s = \langle f_s, 1 \rangle, \quad n_s u_s = \langle f_s, v \rangle, \quad 3n_s K_B T_s = m_s \langle f_s, |v - u_s|^2 \rangle$$

In a similar way, global macroscopic variables such as number density n , density ρ , velocity u and temperature T of the whole mixture are given as follows:

$$\begin{aligned} n &= \sum_{s=1}^L n_s, & \rho &= \sum_{s=1}^L \rho_s, & \rho_s &= m_s n_s, & s &= 1, \dots, L \\ u &= \frac{1}{\rho} \sum_{s=1}^L \rho_s u_s, & 3nK_B T &= 3 \sum_{s=1}^L n_s K_B T_s + \sum_{s=1}^L \rho_s |u_s - u|^2 \end{aligned}$$

2.2. A general consistent BGK model for inert gas mixtures. In [7], authors introduce a BGK-type model (BBGSP model) which prescribes the same exchange rates (2.5) of the binary collision operators Q_{sk} of Boltzmann equation (2.1). In detail, this model uses a relaxation towards fictitious Maxwellian M_{sk} in the place of the binary collision operator Q_{sk} of Boltzmann equation. The model equations are given by

$$(2.7) \quad \frac{\partial f_s}{\partial t} + v \cdot \nabla_x f_s = \frac{1}{\varepsilon} \sum_{k=1}^L \nu_{sk} (n_s M_{sk} - f_s), \quad s = 1, \dots, L$$

where ε is the Knudsen number, $\nu_{sk} > 0$ are free parameters and $M_{sk} := M(v; u_{sk}, \frac{K_B T_{sk}}{m_s})$ are auxiliary Maxwellians depending on fictitious parameter u_{sk} , T_{sk} , which are not the true moments of the distribution functions. In order to guarantee the same exchange rates of the Boltzmann equations, the parameters u_{sk} and T_{sk} take the following forms:

$$(2.8) \quad \begin{aligned} u_{sk} &= (1 - a_{sk})u_s + a_{sk}u_k \\ T_{sk} &= (1 - b_{sk})T_s + b_{sk}T_k + \frac{\gamma_{sk}}{K_B} |u_s - u_k|^2 \end{aligned}$$

with

$$(2.9) \quad a_{sk} = \frac{\lambda_{sk} n_k m_k}{\nu_{sk} (m_s + m_k)}, \quad b_{sk} = \frac{2a_{sk} m_s}{m_s + m_k}, \quad \gamma_{sk} = \frac{m_s a_{sk}}{3} \left(\frac{2m_k}{m_s + m_k} - a_{sk} \right)$$

In spite of the simpler approximate relaxation operator, the model (2.7) still satisfies qualitative properties of Boltzmann equation such as Conservation law, H -theorem, indifferntiability principle. One thing we should keep in mind is that the positivity of T_{sk} should be guaranteed for this model to be well-defined. For this, as remarked in [7], the collision frequency ν_{sk} should satisfy

$$(2.10) \quad \nu_{sk} \geq \frac{1}{2} \lambda_{sk} n_k, \quad \text{given } T_s, T_k > 0.$$

2.2.1. Euler limit. In [4], the Chapman Enskog asymptotic expansion has been formally applied to BGK equations (2.7) in order to obtain proper hydrodynamic closures of the

macroscopic equations. In particular, at zero-th order approximation in the collision dominated regime the following classical Euler system can be obtained:

$$(2.11) \quad \begin{aligned} \frac{\partial n_s}{\partial t} + \nabla_x \cdot (n_s u) &= 0, \quad s = 1, \dots, L \\ \frac{\partial}{\partial t}(\rho u) + \nabla_x \cdot (\rho u \otimes u) + \nabla_x(nK_B T) &= 0, \\ \frac{\partial}{\partial t} \left(\frac{1}{2} \rho |u|^2 + \frac{3}{2} n K_B T \right) + \nabla_x \cdot \left[\left(\frac{1}{2} \rho |u|^2 + \frac{5}{2} n K_B T \right) u \right] &= 0. \end{aligned}$$

2.2.2. Multi-temperature and velocity Euler limit. The structure of the BGK model allows to consider also a hydrodynamic limit where only intra-species collisions are dominant while other inter-species collisions occurs less often. This approach has been described in [5]. We consider the following rescaled form of (2.7):

$$(2.12) \quad \frac{\partial f_s}{\partial t} + v \cdot \nabla_x f_s = \frac{1}{\epsilon} \nu_{ss} (n_s M_{ss} - f_s) + \frac{1}{\kappa} \sum_{k \neq s}^L \nu_{sk} (n_s M_{sk} - f_s).$$

where κ is a positive parameter; it is possible to derive hydrodynamic equations for the macroscopic moments of each species n_s, u_s, T_s . Here we study the behavior of Euler system obtained from (2.12) at zero order when $\epsilon \rightarrow 0$:

$$(2.13) \quad \begin{aligned} \frac{\partial n_s}{\partial t} + \nabla_x \cdot (n_s u_s) &= 0, \\ \frac{\partial}{\partial t}(\rho_s u_s) + \nabla_x \cdot (\rho_s u_s \otimes u_s) + \nabla_x(n_s K_B T_s) &= \frac{1}{\kappa} \sum_{k \neq s}^L \mathcal{R}_{sk}, \\ \frac{\partial}{\partial t} \left(\frac{1}{2} \rho_s |u_s|^2 + \frac{3}{2} n_s K_B T_s \right) + \nabla_x \cdot \left[\left(\frac{1}{2} \rho_s |u_s|^2 + \frac{5}{2} n_s K_B T_s \right) u_s \right] &= \frac{1}{\kappa} \sum_{k \neq s}^L \mathcal{S}_{sk}. \end{aligned}$$

for $s = 1, \dots, L$. The relaxation terms \mathcal{R}_{sk} and \mathcal{S}_{sk} on the r.h.s. are given by

$$(2.14) \quad \begin{aligned} \mathcal{R}_{sk} &= \lambda_{sk} m_{sk} n_s n_k (u_k - u_s), \\ \mathcal{S}_{sk} &= \lambda_{sk} \frac{m_{sk}}{m_s + m_k} n_s n_k [(m_s u_s + m_k u_k) \cdot (u_k - u_s) + 3K_B(T_k - T_s)], \end{aligned}$$

where $m_{sk} = \frac{m_s m_k}{m_s + m_k}$. Note that each gas may have different velocities and temperatures. However, in the limit $\kappa \rightarrow 0$, we can expect that the multi-velocities and temperatures solution of (2.13) will converge to the single velocity and temperature solution of (2.11). This behavior will be checked in Section 6.

Remark 2.1. Multi-temperature Euler equations can be obtained also in the framework of Extended Thermodynamics [25, 28]. Furthermore, the multi-temperature description is able to better reproduce experimental results for mixtures of noble gases, like for instance the shock structure in Helium-Argon mixtures [23].

2.3. Chu reduction. For the solution of the kinetic BGK equations (2.12), it is possible to treat problems in slab geometry, as suitable problems which are 1D in both velocity and space. Indeed, the idea of Chu reduction in [14] enables one to reduce each of the (6+1)-dimensional equation of (2.12) to a pair of two (2+1)-dimensional equations. The system can be derived in case of domains with an axial symmetry with respect to an axis (say x -axis). In such a case, along the other two directions (y and z directions) all gradient

values of distribution functions and macroscopic velocities u_2, u_3 vanish. Considering this and taking moments of (2.12) with respect to $(1, v_2^2 + v_3^2)$, one can obtain the following system:

(2.15)

$$\begin{aligned} \partial_t g_1^s + v \partial_x g_1^s &= \frac{1}{\varepsilon} \nu_{ss} (n_s M_{ss,1} - g_1^s) + \frac{1}{\kappa} \sum_{k \neq s}^L \nu_{sk} (n_s M_{sk,1} - g_1^s), \quad M_{sk,1} = M(v; u_{sk}, \frac{K_B T_{sk}}{m_s}) \\ \partial_t g_2^s + v \partial_x g_2^s &= \frac{1}{\varepsilon} \nu_{ss} (n_s M_{ss,2} - g_2^s) + \frac{1}{\kappa} \sum_{k \neq s}^L \nu_{sk} (n_s M_{sk,2} - g_2^s), \quad M_{sk,2} = \frac{2K_B T_{sk}}{m_s} M_{sk,1}, \end{aligned}$$

where

$$g_1^s(t, x, v) = \int_{\mathbb{R}} f(t, x, v) dv_2 dv_3, \quad g_2^s(t, x, v) = \int_{\mathbb{R}} (v_2^2 + v_3^2) f(t, x, v) dv_2 dv_3$$

Here the first component of velocity variable is denoted by $v \equiv v_1$. We remark that the macroscopic quantities in (2.15) can be computed as in (2.6). Using

$$n_s = \int_{\mathbb{R}} g_1^s dv, \quad n_s u_s = \int_{\mathbb{R}} v g_1^s dv, \quad \frac{3n_s K_B T_s}{2m_s} = \int_{\mathbb{R}} \frac{|v - u_s|^2}{2} g_1^s + \frac{g_2^s}{2} dv,$$

with (2.8) and (2.9), one can compute u_{sk} and T_{sk} from g_1^s and g_2^s .

Based on the Chu reduction, our numerical schemes and simulations will be focused on the one-dimensional problem in space. To avoid confusion, we end this section with the representation of one-dimensional hydrodynamic models we will use in the rest of this paper:

- (1) One-dimensional single velocity and temperature Euler system for (2.11):

$$\begin{aligned} (2.16) \quad & \frac{\partial n_s}{\partial t} + \partial_x (n_s u) = 0, \quad s = 1, \dots, L \\ & \frac{\partial}{\partial t} (\rho u) + \partial_x (\rho u^2 + n K_B T) = 0, \\ & \frac{\partial}{\partial t} \left(\frac{1}{2} \rho |u|^2 + \frac{3}{2} n K_B T \right) + \partial_x \left[\left(\frac{1}{2} \rho |u|^2 + \frac{5}{2} n K_B T \right) u \right] = 0. \end{aligned}$$

- (2) One-dimensional multi velocities and temperatures Euler system for (2.13):

$$\begin{aligned} (2.17) \quad & \frac{\partial n_s}{\partial t} + \partial_x (n_s u_s) = 0, \\ & \frac{\partial}{\partial t} (\rho_s u_s) + \partial_x (\rho_s u_s^2 + n_s K_B T_s) = \frac{1}{\kappa} \sum_{k \neq s}^L \mathcal{R}_{sk}, \\ & \frac{\partial}{\partial t} \left(\frac{1}{2} \rho_s |u_s|^2 + \frac{3}{2} n_s K_B T_s \right) + \partial_x \left[\left(\frac{1}{2} \rho_s |u_s|^2 + \frac{5}{2} n_s K_B T_s \right) u_s \right] = \frac{1}{\kappa} \sum_{k \neq s}^L \mathcal{S}_{sk}, \end{aligned}$$

for $s = 1, \dots, L$. Here \mathcal{R}_{sk} and \mathcal{S}_{sk} are computed as in (2.14)

3. SEMI-LAGRANGIAN METHODS FOR A GENERAL CONSISTENT BGK MODEL

In this section, we propose a semi-Lagrangian method (SL) in the finite difference framework for solving (2.12). The SL approach has been adopted for various BGK-type models in the context of single gas BGK model [8, 13, 17, 26] or ES-BGK type models [9, 27] and a gas mixture model [18]. The main advantage of the technique is to avoid both CFL-type

time step restriction of convection term and the stiffness arising in the hydrodynamic limit $\varepsilon \rightarrow 0$.

In the following description, we assume a fixed time step Δt and uniform mesh sizes Δx , Δv for space and velocity, respectively. The corresponding grid points will be denoted by

$$\begin{aligned} t_n &= n\Delta t, & n &= 0, 1, \dots, N_t \\ v_j &= v_{min} + (j-1)\Delta v, & j &= 1, 2, \dots, N_v + 1 \end{aligned}$$

where $N_t\Delta t$ reproduces the final time t_f for computation, $[v_1, v_{N_v+1}]$ recovers the velocity domain $[v_{min}, v_{max}]$. For space, we assign grid points x_i in different ways:

- for periodic boundary condition:

$$(3.1) \quad x_i = x_0 + (i-1)\Delta x, i = 1, \dots, N_x.$$

- for free-flow boundary condition:

$$(3.2) \quad x_i = x_0 + \left(i - \frac{1}{2}\right)\Delta x, i = 1, \dots, N_x.$$

For the description of numerical methods, we use the following notation. For $s = 1, \dots, L$, we define discrete quantities as follows:

- Numerical solutions for s -species gas:

$$g_{1,ij}^{s,n+1} \approx g_1^s(t^{n+1}, x_i, v_j), \quad g_{2,ij}^{s,n+1} \approx g_2^s(t^{n+1}, x_i, v_j).$$

- Discrete macroscopic moments for s -species gas:

$$(3.3) \quad \begin{aligned} n_{s,i}^{n+1} &:= \sum_j g_{1,ij}^{s,n+1} \Delta v, \\ n_{s,i}^{n+1} u_{s,i}^{n+1} &:= \sum_j v_j g_{1,ij}^{s,n+1} \Delta v, \\ \frac{3n_{s,i}^{n+1} K_B T_i^{n+1}}{2m_s} &:= \sum_j g_{1,ij}^{s,n+1} \frac{(v_j - u_{s,i}^{n+1})^2}{2} \Delta v + \sum_j \frac{g_{2,ij}^{s,n+1}}{2} \Delta v. \end{aligned}$$

- Collision frequencies

$$\nu_{sk,i}^n \approx \nu_{sk}(t^n, x_i)$$

- Auxiliary parameters

$$(3.4) \quad \begin{aligned} a_{sk,i}^n &= \frac{\lambda_{sk} n_{k,i}^n m_k}{\nu_{sk,i}^n (m_s + m_k)}, \quad b_{sk,i}^n = \frac{2a_{sk,i}^{n+1} m_s}{m_s + m_k}, \quad \gamma_{sk,i}^n = \frac{m_i a_{sk,i}^{n+1}}{3} \left(\frac{2m_k}{m_s + m_k} - a_{sk,i}^{n+1} \right), \\ u_{sk,i}^n &= (1 - a_{sk,i}^n) u_{s,i}^n + a_{sk,i}^n u_{k,i}^n, \\ T_{sk,i}^n &= (1 - b_{sk,i}^n) T_{s,i}^n + b_{sk,i}^n T_{k,i}^n + \frac{\gamma_{sk,i}^n}{K_B} (u_{s,i}^n - u_{k,i}^n)^2. \end{aligned}$$

3.1. Derivation of a first order SL scheme. Semi-Lagrangian schemes for (2.15) can be derived by treating the equation in the Lagrangian formation:

$$(3.5) \quad \frac{dg_p^s}{dt} = \frac{1}{\varepsilon} \nu_{ss} (n_s M_{ss,p} - g_p^s) + \frac{1}{\kappa} \sum_{k \neq s}^L \nu_{sk} (n_s M_{sk,p} - g_p^s), \quad g_p^s(0, x, v) = g_{p,0}^s(\tilde{x}, v)$$

$$(3.6) \quad \frac{dx}{dt} = v, \quad x(0) = \tilde{x}$$

where $g_{p,0}^s(x, v)$ is the initial condition and $M_{sk,p}$ are given in (2.15). Here the analytic solution to (3.6) is a characteristic curve passing through the position x with velocity v at time t . Tracing back along characteristic curve, we reach the location \tilde{x} and we call this *characteristic foot*.

A first order implicit scheme can be obtained by applying implicit Euler method to (3.6):

(3.7)

$$g_{1,ij}^{s,n+1} = \tilde{g}_{1,ij}^{s,n} + \frac{\Delta t}{\varepsilon} \nu_{ss,i}^{n+1} \left(n_{s,i}^{n+1} M_{ss,1,ij}^{n+1} - g_{1,ij}^{s,n+1} \right) + \frac{\Delta t}{\kappa} \sum_{k \neq s}^L \nu_{sk,i}^{n+1} \left(n_{s,i}^{n+1} M_{sk,1,ij}^{n+1} - g_{1,ij}^{s,n+1} \right),$$

(3.8)

$$g_{2,ij}^{s,n+1} = \tilde{g}_{2,ij}^{s,n} + \frac{\Delta t}{\varepsilon} \nu_{ss,i}^{n+1} \left(n_{s,i}^{n+1} M_{ss,2,ij}^{n+1} - g_{2,ij}^{s,n+1} \right) + \frac{\Delta t}{\kappa} \sum_{k \neq s}^L \nu_{sk,i}^{n+1} \left(n_{s,i}^{n+1} M_{sk,2,ij}^{n+1} - g_{2,ij}^{s,n+1} \right).$$

From the first equation, one can obtain

$$(3.9) \quad n_{s,i}^{n+1} = \sum_j \tilde{g}_{1,ij}^{s,n+1} \Delta v =: \tilde{n}_{s,i}^{n+1},$$

Using this, we get

$$(3.10) \quad \nu_{sk,i}^{n+1} = \lambda_{sk} n_{k,i}^{n+1} = \lambda_{sk} \tilde{n}_{k,i}^n = \tilde{\nu}_{sk,i}^n,$$

and

$$(3.11) \quad \begin{aligned} a_{sk,i}^{n+1} &= \frac{\lambda_{sk} n_{k,i}^{n+1} m_k}{\nu_{sk,i}^{n+1} (m_s + m_k)} = \frac{\lambda_{sk} \tilde{n}_{k,i}^n m_k}{\tilde{\nu}_{sk,i}^n (m_s + m_k)} =: \tilde{a}_{sk,i}^n, \\ b_{sk,i}^{n+1} &= \frac{2a_{sk,i}^{n+1} m_s}{m_s + m_k} = \frac{2\tilde{a}_{sk,i}^n m_s}{m_s + m_k} =: \tilde{b}_{sk,i}^n, \\ \gamma_{sk,i}^{n+1} &= \frac{m_s a_{sk,i}^{n+1}}{3} \left(\frac{2m_k}{m_s + m_k} - a_{sk,i}^{n+1} \right) = \frac{m_s \tilde{a}_{sk,i}^n}{3} \left(\frac{2m_k}{m_s + m_k} - \tilde{a}_{sk,i}^n \right) =: \tilde{\gamma}_{sk,i}^n \end{aligned}$$

To compute $u_{sk,ij}^{n+1}$, we consider

$$\begin{aligned} n_{s,i}^{n+1} u_{s,i}^{n+1} &= \sum_j v_j g_{1,ij}^{s,n+1} \Delta v \\ &= \sum_j v_j \left(\tilde{g}_{1,ij}^{s,n} + \frac{\Delta t}{\varepsilon} \nu_{ss,i}^{n+1} \left(n_{s,i}^{n+1} M_{ss,1,ij}^{n+1} - g_{1,ij}^{s,n+1} \right) + \frac{\Delta t}{\kappa} \sum_{k \neq s}^L \nu_{sk,i}^{n+1} \left(n_{s,i}^{n+1} M_{sk,1,ij}^{n+1} - g_{1,ij}^{s,n+1} \right) \right) \Delta v, \end{aligned}$$

which can be rewritten as

$$n_{s,i}^{n+1} u_{s,i}^{n+1} = \tilde{n}_{s,i}^n \tilde{u}_{s,i}^n + \frac{\Delta t}{\kappa} \sum_{k \neq s}^L \nu_{sk,i}^{n+1} \left(n_{s,i}^{n+1} u_{sk,i}^{n+1} - n_{s,i}^{n+1} u_{s,i}^{n+1} \right).$$

This, together with (3.9) and (3.10), gives

$$u_{s,i}^{n+1} = \tilde{u}_{s,i}^n + \frac{\Delta t}{\kappa} \sum_{k \neq s}^L \tilde{\nu}_{sk,i}^n \left(u_{sk,i}^{n+1} - u_{s,i}^{n+1} \right).$$

Now, we recall (3.4) to get

$$(3.12) \quad u_{sk,i}^{n+1} = (1 - a_{sk,i}^{n+1}) u_{s,i}^{n+1} + a_{sk,i}^{n+1} u_{k,i}^{n+1},$$

and use this to obtain

$$\begin{aligned} u_{s,i}^{n+1} &= \tilde{u}_{s,i}^n + \frac{\Delta t}{\kappa} \sum_{k \neq s}^L \tilde{\nu}_{sk,i}^n \left((1 - a_{sk,i}^{n+1}) u_{s,i}^{n+1} + a_{sk,i}^{n+1} u_{k,i}^{n+1} - u_{s,i}^{n+1} \right) \\ &= \tilde{u}_{s,i}^n - \frac{\Delta t}{\kappa} \sum_{k=1}^L \tilde{\nu}_{sk,i}^n a_{sk,i}^{n+1} \left(u_{s,i}^{n+1} - u_{k,i}^{n+1} \right). \end{aligned}$$

This combined with the relation (3.11) gives

$$(3.13) \quad u_{s,i}^{n+1} + \frac{\Delta t}{\kappa} \sum_{k \neq s}^L \tilde{\nu}_{sk,i}^n \tilde{a}_{sk,i}^n \left(u_{s,i}^{n+1} - u_{k,i}^{n+1} \right) = \tilde{u}_{s,i}^n,$$

which can be rewritten as

$$(3.14) \quad \underline{A}_i^n \underline{u}_i^{n+1} = \tilde{\underline{u}}_i^n,$$

where the (s, k) entry of the $s \times s$ matrix \underline{A}_i^n is given by

$$\underline{A}_{i,sk}^n = \begin{cases} 1 + \frac{\Delta t}{\kappa} \sum_{k \neq s}^L \tilde{\nu}_{sk,i}^n \tilde{a}_{sk,i}^n, & \text{if } s = k \\ -\frac{\Delta t}{\kappa} \tilde{\nu}_{sk,i}^n \tilde{a}_{sk,i}^n, & \text{if } s \neq k \end{cases}$$

with

$$\underline{u}_i^{n+1} := (u_{1,i}^{n+1}, u_{2,i}^{n+1}, \dots, u_{L,i}^{n+1})^\top, \quad \tilde{\underline{u}}_i^n := (\tilde{u}_{1,i}^n, \tilde{u}_{2,i}^n, \dots, \tilde{u}_{L,i}^n)^\top.$$

We note that the matrix \underline{A}_i^n is always invertible because we have

$$|\underline{A}_{i,ss}^n| > \sum_{k \neq s}^L |\underline{A}_{i,sk}^n|, \quad \text{for every } s = 1 \dots, L.$$

Solving (3.14), we obtain $u_{s,i}^{n+1}$.

To compute $T_{s,i}^{n+1}$ explicitly, we take a summation (3.7) w.r.t. $|v_j - u_{s,i}^{n+1}|^2/2$ and (3.8) w.r.t. $1/2$, respectively. Then, we sum these to obtain

$$(3.15) \quad \begin{aligned} &\frac{3n_{s,i}^{n+1} K_B T_{s,i}^{n+1}}{2m_s} - \frac{3\tilde{n}_{s,i}^n K_B \tilde{T}_{s,i}^n}{2m_s} - \frac{\tilde{n}_{s,i}^n}{2} (u_{s,i}^{n+1} - \tilde{u}_{s,i}^n)^2 \\ &= \frac{\Delta t}{\kappa} \sum_{k \neq s}^L \nu_{sk,i}^{n+1} \left(\frac{3n_{s,i}^{n+1} K_B T_{sk,i}^{n+1}}{2m_s} + \frac{n_{s,i}^{n+1}}{2} (u_{sk,i}^{n+1} - u_{s,i}^{n+1})^2 - \frac{3n_{s,i}^{n+1} K_B T_{s,i}^{n+1}}{2m_s} \right). \end{aligned}$$

Using (3.9) and (3.10), we get

$$T_{s,i}^{n+1} = \tilde{T}_{s,i}^n + \frac{m_s}{3K_B} (u_{s,i}^{n+1} - \tilde{u}_{s,i}^n)^2 + \frac{\Delta t}{\kappa} \sum_{k \neq s}^L \tilde{\nu}_{sk,i}^n \left(T_{sk,i}^{n+1} + \frac{m_s}{3K_B} (u_{sk,i}^{n+1} - u_{s,i}^{n+1})^2 - T_{s,i}^{n+1} \right).$$

Now, we use the relation (3.4) to get

$$T_{sk,i}^{n+1} = (1 - b_{sk,i}^{n+1}) T_{s,i}^{n+1} + b_{sk,i}^{n+1} T_{k,i}^{n+1} + \frac{\gamma_{sk,i}^{n+1}}{K_B} (u_{s,i}^{n+1} - u_{k,i}^{n+1})^2.$$

This, combined with (3.12), gives

$$\begin{aligned} T_{s,i}^{n+1} &= \tilde{T}_{s,i}^n + \frac{m_s}{3K_B} (u_{s,i}^{n+1} - \tilde{u}_{s,i}^n)^2 \\ &\quad + \frac{\Delta t}{\kappa} \sum_{k \neq s}^L \tilde{\nu}_{sk,i}^n \left(b_{sk,i}^{n+1} (-T_{s,i}^{n+1} + T_{k,i}^{n+1}) + \left(\frac{\tilde{\gamma}_{sk,i}^{n+1}}{K_B} + \frac{m_s}{3K_B} (a_{sk,i}^{n+1})^2 \right) (u_{s,i}^{n+1} - u_{k,i}^{n+1})^2 \right). \end{aligned}$$

Using (3.11), we can also derive

$$\begin{aligned} (3.16) \quad T_{s,i}^{n+1} &+ \frac{\Delta t}{\kappa} \sum_{k \neq s}^L \tilde{\nu}_{sk,i}^n \tilde{b}_{sk,i}^n (T_{s,i}^{n+1} - T_{k,i}^{n+1}) \\ &= \tilde{T}_{s,i}^n + \frac{m_s}{3K_B} (u_{s,i}^{n+1} - \tilde{u}_{s,i}^n)^2 + \frac{\Delta t}{\kappa} \sum_{k \neq s}^L \tilde{\nu}_{sk,i}^n \left(\frac{\tilde{\gamma}_{sk,i}^n}{K_B} + \frac{m_s}{3K_B} (\tilde{a}_{sk,i}^n)^2 \right) (u_{s,i}^{n+1} - u_{k,i}^{n+1})^2 \end{aligned}$$

This system also reduces to a solvable linear system:

$$\underline{B}_i^n \underline{T}_i^{n+1} = \tilde{\xi}_i^n,$$

where

$$B_{sk} = \begin{cases} 1 + \frac{\Delta t}{\kappa} \sum_{k \neq s}^L \tilde{\nu}_{sk,i}^n \tilde{b}_{sk,i}^n, & \text{if } s = k \\ -\frac{\Delta t}{\kappa} \tilde{\nu}_{sk,i}^n \tilde{b}_{sk,i}^n, & \text{if } s \neq k \end{cases}$$

$$\underline{T}_i^{n+1} := (T_{1,i}^{n+1}, T_{2,i}^{n+1}, \dots, T_{L,i}^{n+1})^\top,$$

$$\tilde{\xi}_i^n := (\tilde{\xi}_{1,i}^n, \tilde{\xi}_{2,i}^n, \dots, \tilde{\xi}_{L,i}^n)^\top,$$

$$\tilde{\xi}_{s,i}^n := \tilde{T}_{s,i}^n + \frac{m_s}{3K_B} (u_{s,i}^{n+1} - \tilde{u}_{s,i}^n)^2 + \frac{\Delta t}{\kappa} \sum_{k \neq s}^L \tilde{\nu}_{sk,i}^n \left(\frac{\tilde{\gamma}_{sk,i}^n}{K_B} + \frac{m_s}{3K_B} (\tilde{a}_{sk,i}^n)^2 \right) (u_{s,i}^{n+1} - u_{k,i}^{n+1})^2.$$

Since (3.13) and (3.16) allows one to compute $u_{s,i}^{n+1}$ and $T_{s,i}^{n+1}$ explicitly, it also gives

$$M_{sk,1,ij}^{n+1} = M(v; u_{sk,i}^{n+1}, \frac{K_B T_{sk,i}^{n+1}}{m_s}), \quad M_{sk,2,ij}^{n+1} = 2 \frac{K_B T_{sk,i}^{n+1}}{m_s} M_{sk,1,ij}^{n+1}$$

Then, our numerical solution reads

$$(3.17) \quad g_{p,ij}^{s,n+1} = \frac{\tilde{g}_{p,ij}^{s,n} + \frac{\Delta t}{\varepsilon} \nu_{ss,i}^{n+1} n_{s,i}^{n+1} M_{ss,p,ij}^{n+1} + \frac{\Delta t}{\kappa} \sum_{k \neq s}^L \nu_{sk,i}^{n+1} n_{s,i}^{n+1} M_{sk,p,ij}^{n+1}}{1 + \frac{\Delta t}{\varepsilon} \nu_{ss,i}^{n+1} + \frac{\Delta t}{\kappa} \sum_{k \neq s}^L \nu_{sk,i}^{n+1}},$$

where $p = 1, 2$.

Algorithm of first order SL scheme.

- (1) Reconstruct $\tilde{g}_{p,ij}^{s,n}$ at $x_i - v_j \Delta t$ from $\{g_{p,ij}^{s,n}\}$.
- (2) Compute $\tilde{n}_i^n, \tilde{u}_i^n, \tilde{T}_{s,i}^n, \tilde{\nu}_{sk,i}^n, \tilde{a}_i^n, \tilde{b}_i^n, \tilde{\gamma}_i^n$ from $\{\tilde{g}_{p,ij}^{s,n}\}$,
- (3) Compute $n_i^{n+1}, u_i^{n+1}, T_{s,i}^{n+1}, \nu_{sk,i}^{n+1}, a_i^{n+1}, b_i^{n+1}, \gamma_i^{n+1}$ with $\tilde{n}_i^n, \tilde{u}_i^n, \tilde{T}_{s,i}^n, \tilde{\nu}_{sk,i}^n, \tilde{a}_i^n, \tilde{b}_i^n, \tilde{\gamma}_i^n$
- (4) Construct $M_{sk,p,ij}^{n+1}$
- (5) Update solutions with (3.17).

Remark 3.1. When we reconstruct solutions on the characteristic feet, the linear interpolation will be sufficient to achieve first order accuracy.

4. HIGH ORDER SEMI-LAGRANGIAN METHODS

4.1. Time discretization. In this section, we present high order SL schemes for (2.15) by applying L-stable diagonally implicit Runge-Kutta methods (DIRK) or backward difference formula methods (BDF) with high order spatial reconstructions. High order methods can be derived as in the first order scheme, so we only present its algorithm.

4.1.1. *DIRK methods.* DIRK methods can be represented by Butcher's table [20]:

$$\frac{c}{\mid} \frac{A}{b^\top}$$

where A is a $s \times s$ lower triangle matrix whose diagonal entries are non-zero constant, $c = (c_1, \dots, c_s)^\top$ and $b = (b_1, \dots, b_s)^\top$ are coefficients vectors with $c_i = \sum_{j=1}^s a_{ij}$, for $i = 1, \dots, s$. In this paper, we use for numerical simulations the following two DIRK methods adopted in [17]:

$$(4.1) \quad \text{DIRK2} = \frac{\alpha \mid \begin{array}{cc} \alpha & 0 \\ 1 - \alpha & \alpha \\ 1 - \alpha & \alpha \end{array}}{1}, \quad \text{DIRK3} = \frac{\begin{array}{ccc} \gamma & \gamma & 0 & 0 \\ \frac{1+\gamma}{2} & \frac{1-\gamma}{2} & \gamma & 0 \\ 1 & 1 - \delta - \gamma & \delta & \gamma \end{array}}{1 - \delta - \gamma \mid \begin{array}{cc} \delta & \gamma \\ \delta & \gamma \end{array}}$$

where $\alpha = 1 - \frac{\sqrt{2}}{2}$, $\gamma = 0.4358665215$ and $\delta = -0.644363171$. For simplicity, we introduce the following notations:

- Consider a backward-characteristic which comes from x_i with v_j at time $t^n + c_m \Delta t$. We call this m th characteristic. Then, the location of its characteristic at the ℓ th stage is given by :

$$x_{i,j}^{m,\ell} := x_i - (c_m - c_\ell)v_j \Delta t$$

Note that $x_{i,j}^{m,m} = x_i$.

- For $p = 1, 2$, the ℓ th stage value of the distribution function along the m th backward-characteristic which comes from x_i with v_j at time $t^n + c_\ell \Delta t$ is given by :

$$g_{p,ij}^{s,(m,\ell)} := g_p^s(x_{i,j}^{m,\ell}, v_j, t^n + c_\ell \Delta t).$$

- For $p = 1, 2$, let us define K_p^s by

$$K_p^s := \frac{1}{\varepsilon} \nu_{ss} (n_s M_{ss,p} - g_p^s) + \frac{1}{\kappa} \sum_{k \neq s}^L \nu_{sk} (n_s M_{sk,p} - g_p^s).$$

- For $p = 1, 2$, the ℓ -th stage value of K_p^s along the m -th backward-characteristic which comes from x_i with v_j at time $t^n + c_\ell \Delta t$:

$$K_{p,ij}^{s,(m,\ell)} := K_p^s(x_{i,j}^{m,\ell}, v_j, t^n + c_\ell \Delta t).$$

Using the same argument of the first order SL scheme, all computations for ν -stage DIRK based SL methods can be performed explicitly. For $p = 1, 2$, let us consider m -stage values

of g_p^s :

$$\begin{aligned}
(4.2) \quad g_{p,ij}^{s,(m,m)} &= \tilde{g}_{p,ij}^{s,(m,0)} + \Delta t \sum_{\ell=1}^{m-1} a_{m\ell} K_{p,ij}^{s,(m,\ell)} \\
&+ \frac{\Delta t}{\varepsilon} a_{mm} \nu_{ss,ij}^{(m,m)} \left(n_{s,i}^{(m,m)} M_{ss,p,ij}^{(m,m)} - g_{1,ij}^{s,(m,m)} \right) \\
&+ \frac{\Delta t}{\kappa} \sum_{k \neq s}^L a_{mm} \nu_{sk,ij}^{(m,m)} \left(n_{s,i}^{(m,m)} M_{sk,p,ij}^{(m,m)} - g_{1,ij}^{s,(m,m)} \right)
\end{aligned}$$

In case of $\nu = 1$, the implicit Euler method has $a_{11} = 1$, and one can update solution with the scheme (3.17).

In case of $\nu > 1$, the computation of m -stage value $g_{p,ij}^{s,(m,m)}$, can be understood as repetition of the first order method. However, one should be careful in that the term, $\tilde{g}_{p,ij}^{s,(m,0)} + \Delta t \sum_{\ell=1}^{m-1} a_{m\ell} K_{p,ij}^{s,(m,\ell)}$, now plays the of $\tilde{g}_{p,ij}^{s,n}$ and the coefficient of Δt is multiplied by a_{mm} . We also note that reconstructions of g and K on characteristic feet will be necessary. To sum up, DIRK based methods can be updated as follows:

Algorithm of ν -stage DIRK based SL scheme.

- (1) Reconstruct $\tilde{g}_{p,ij}^{s,(m,0)}$ at $x_i - v_j c_m \Delta t$ from $\{g_{p,ij}^{s,n}\}$.
- (2) Compute $\tilde{g}_{p,ij}^{s,m,*} := \tilde{g}_{p,ij}^{s,(m,0)} + \Delta t \sum_{\ell=1}^{m-1} a_{m\ell} K_{p,ij}^{s,(m,\ell)}$.
- (3) Compute $\tilde{n}_i^{m,*}, \tilde{u}_i^{m,*}, \tilde{T}_{s,i}^{m,*}, \tilde{\nu}_{sk,i}^{m,*}, \tilde{a}_i^{m,*}, \tilde{b}_i^{m,*}, \tilde{\gamma}_i^{m,*}$ from $\{\tilde{g}_{p,ij}^{s,m,*}\}$
- (4) Compute $n_i^{(m,m)}, u_i^{(m,m)}, T_{s,i}^{(m,m)}, \nu_{sk,i}^{(m,m)}, a_i^{(m,m)}, b_i^{(m,m)}, \gamma_i^{(m,m)}$ with $\tilde{n}_i^{m,*}, \tilde{u}_i^{m,*}, \tilde{T}_{s,i}^{m,*}, \tilde{\nu}_{sk,i}^{m,*}, \tilde{a}_i^{m,*}, \tilde{b}_i^{m,*}, \tilde{\gamma}_i^{m,*}$
- (5) Construct $M_{sk,p,ij}^{(m,m)}$
- (6) Update solutions with (4.2).

Remark 4.1.

- (1) For high order spatial reconstruction, we adopt a conservative reconstruction presented in [12, 13].
- (2) We note that the relation (4.2) is linear because we explicitly precompute $M_{sk,p,ij}^{(m,m)}$ before computing $g_{p,ij}^{s,(m,m)}$.
- (3) We compute numerical solutions by the last stage value $g_{p,ij}^{s,n+1} = g_{p,ij}^{s,(\nu,\nu)}$ because we consider stiffly accurate DIRK schemes.

4.1.2. BDF methods. An efficient class of high order SL schemes can be designed with linear multi-step methods such as Backward difference formula (BDF) in [20]. The BDF method of order s is represented by

$$(4.3) \quad BDF : y^{n+1} = \sum_{k=1}^s \alpha_k y^{n+1-k} + \beta_s \Delta t g(y^{n+1}, t_{n+1}).$$

where α_k and β_s are constants depending on s . In particular, we are to use second and third order methods:

$$\begin{aligned}
(4.4) \quad BDF2 : \alpha_1 &= \frac{4}{3}, \quad \alpha_2 = -\frac{1}{3}, \quad \beta_2 = \frac{2}{3}, \\
BDF3 : \alpha_1 &= \frac{18}{11}, \quad \alpha_2 = -\frac{9}{11}, \quad \alpha_3 = \frac{2}{11}, \quad \beta_3 = \frac{6}{11}
\end{aligned}$$

For BDF based methods, we use the following notation:

- In case of BDF methods, we consider a backward-characteristic which comes from x_i with v_j at time t^{n+1} . Along this characteristic, its characteristic foot at time t^{n+1-k} will be located at $x_{i,j}^k := x_i - kv_j\Delta t$ for $k = 1, \dots, s$.
- For $p = 1, 2$, the value of distribution functions located on $x_{i,j}^k$ at time t^{n+1-k} along the backward-characteristic corresponding to x_i with v_j will be denoted by

$$g_{p,ij}^{s,n+1-k} := g_p^s(x_{i,j}^k, v_j, t^{n+1-k}).$$

- For $p = 1, 2$, the ℓ -th stage value of K_p^s along the m -th backward-characteristic which comes from x_i with v_j at time $t^n + c_k\Delta t$:

$$K_{p,ij}^{s,n+1-k} := K_p^s(x_{i,j}^k, v_j, t^{n+1-k}).$$

With s -order BDF methods, the SL scheme reads

$$(4.5) \quad \begin{aligned} g_{p,ij}^{s,n+1} &= \sum_{k=1}^{\nu} \alpha_k \tilde{g}_{p,ij}^{s,n+1-k} + \frac{\Delta t}{\varepsilon} \beta_{\nu} \nu_{sk,i}^{n+1} \left(n_{s,i}^{n+1} M_{sk,p,ij}^{n+1} - g_{p,ij}^{s,n+1} \right) \\ &+ \frac{\Delta t}{\kappa} \sum_{k \neq s}^L \beta_{\nu} \nu_{sk,i}^{n+1} \left(n_{s,i}^{n+1} M_{sk,p,ij}^{n+1} - g_{p,ij}^{s,n+1} \right). \end{aligned}$$

Algorithm of s -order BDF based SL scheme.

- (1) Reconstruct $\tilde{g}_{p,ij}^{s,n+1-k}$ at $x_{i,j}^k := x_i - kv_j\Delta t$ from $\{g_{p,ij}^{s,n+1-k}\}$.
- (2) Compute $\tilde{g}_{p,ij}^{s,*} := \sum_{k=1}^s \alpha_k \tilde{g}_{p,ij}^{s,n+1-k} + \frac{\Delta t}{\varepsilon} \beta_s \nu_{sk,i}^{n+1} \left(n_{s,i}^{n+1} M_{sk,p,ij}^{n+1} - g_{p,ij}^{s,n+1} \right)$.
- (3) Compute $\tilde{n}_i^*, \tilde{u}_i^*, \tilde{T}_{s,i}^*, \tilde{\nu}_{sk,i}^*, \tilde{a}_i^*, \tilde{b}_i^*, \tilde{\gamma}_i^*$ from $\{\tilde{g}_{p,ij}^{s,*}\}$.
- (4) Compute $n_i^{n+1}, u_i^{n+1}, T_{s,i}^{n+1}, \nu_{sk,i}^{n+1}, a_i^{n+1}, b_i^{n+1}, \gamma_i^{n+1}$ with $\tilde{n}_i^*, \tilde{u}_i^*, \tilde{T}_{s,i}^*, \tilde{\nu}_{sk,i}^*, \tilde{a}_i^*, \tilde{b}_i^*, \tilde{\gamma}_i^*$.
- (5) Construct $M_{sk,p,ij}^{n+1}$.
- (6) Update solutions with (4.5).

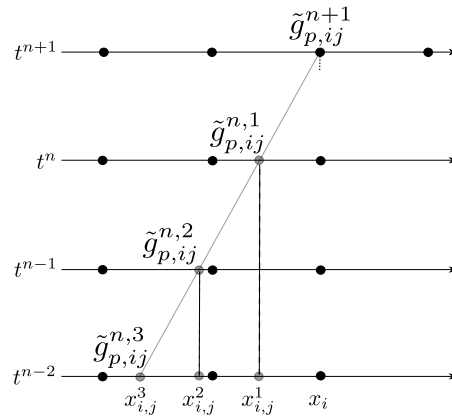


FIGURE 1. BDF3 based SL method. On grey points, $\tilde{g}_{p,ij}^{n,k}$ will be reconstructed for each $k = 1, 2, 3$ and $p = 1, 2$ from $\{g_{p,ij}^{n+1-k}\}$.

In Figure 1, we describe the schematic of BDF3 based SL scheme. Note that a characteristic starting from position x_i with velocity v_j at time t^{n+1} passes through three points $x_{i,j}^k$, $k = 1, 2, 3$ where reconstructions are necessary.

5. CONSERVATIVE RECONSTRUCTION

In this section, we briefly present a conservative reconstruction technique introduced in [12, 13]. The main idea of the approach is to take a sliding average of a basic reconstruction. As in literatures [12, 13], we also take CWENO reconstructions as basic reconstructions. In the following description, we consider two cases $k = 2, 4$, which correspond to CWENO23 [22] and CWENO35 [15], respectively. We summarize the procedure of the conservative reconstruction as follows:

- (1) Given point-wise values $\{u_i\}$ on grid points $\{x_i\}$, compute a CWENO reconstruction for each cell $I_i = [x_i - \Delta x/2, x_i + \Delta x/2]$:

$$R_i(x) = \sum_{\ell=0}^k \frac{R_i^{(\ell)}}{\ell!} (x - x_i)^\ell.$$

This yields a CWENO reconstruction on the spatial domain:

$$R(x) = \sum_i R_i(x) \chi_i(x),$$

where $\chi_i(x)$ is an indicator function defined on cell I_i .

- (2) For any $\theta \in [0, 1]$, approximate $u(x_i + \theta \Delta x)$ by $Q(x_i + \theta \Delta x)$:

$$u(x_i + \theta \Delta x) \approx Q(x_i + \theta \Delta x) := \frac{1}{\Delta x} \int_{x_i + \theta \Delta x - \Delta x/2}^{x_i + \theta \Delta x - \Delta x/2} R(y) dy$$

whose explicit form is given by

$$Q(x_i + \theta \Delta x) = \sum_{\ell=0}^k (\Delta x)^\ell \left(\alpha_\ell(\theta) R_i^{(\ell)} + \beta_\ell(\theta) R_{i+1}^{(\ell)} \right),$$

where

$$\alpha_\ell(\theta) = \frac{1 - (2\theta - 1)^{\ell+1}}{2^{\ell+1}(\ell + 1)!}, \quad \beta_\ell(\theta) = \frac{(2\theta - 1)^{\ell+1} - (-1)^{\ell+1}}{2^{\ell+1}(\ell + 1)!}.$$

In the following section, the resulting conservative reconstruction based on CWENO23 ($k = 2$) will be denoted by Q-CWENO23. Similarly, we call the conservative reconstruction based on CWENO35 ($k = 4$) by Q-CWENO35.

6. NUMERICAL TESTS

In this section, we verify the performance of high-order conservative semi-Lagrangian methods to (2.15). For tests, we use high order schemes dealt with in sections 4-5. In particular, we consider the following combination of time integration methods and spatial reconstructions:

- (1) RK2-QCW23: DIRK2 with Q-CWENO23.
- (2) RK3-QCW35: DIRK3 with Q-CWENO35.
- (3) BDF2-QCW23: BDF2 with Q-CWENO23.
- (4) BDF3-QCW35: BDF3 with Q-CWENO35.

Here the Q-CWENO23 and Q-CWENO35 reconstructions are high order conservative reconstruction adopted in [12, 13]. Throughout this section, we determine a time step Δt based on the CFL number defined by

$$\text{CFL} = \max_j |v_j| \frac{\Delta t}{\Delta x}.$$

Considering the relation in (2.10), throughout numerical experiments we consider collision frequencies of the following form: $\nu_{sk} = \lambda_{sk} n_k$ which will be divided by ε or κ .

6.1. Accuracy test. As in [1, 18], we consider gas mixtures of four monoatomic gases whose molecular masses are given by

$$m_1 = 58.5, \quad m_2 = 18, \quad m_3 = 40, \quad m_4 = 36.5.$$

The values of λ_{sk} are:

$$(6.1) \quad \begin{array}{cccc} \lambda_{11} = 5, & \lambda_{12} = 6, & \lambda_{13} = 2, & \lambda_{14} = 7 \\ & \lambda_{22} = 4, & \lambda_{23} = 5, & \lambda_{24} = 8 \\ & & \lambda_{33} = 4, & \lambda_{34} = 3 \\ & & & \lambda_{44} = 6, \end{array}$$

where $\lambda_{sk} = \lambda_{ks}$ for $s, k = 1, \dots, 4$. Here we set $\kappa = \varepsilon$. We take as initial data Maxwellians whose macroscopic fields are

$$(6.2) \quad \begin{aligned} n_0^s(x) &= \frac{1}{m_s}, \quad T_0^s(x) = \frac{4}{\sum_{s=1}^4 n_0^s}, \\ u_0^s(x) &= \frac{s}{\sigma_s} \left[\exp \left(- \left(\sigma_s x - 1 + \frac{s}{3} \right)^2 \right) + \exp \left(- \left(\sigma_s x + 3 - \frac{s}{10} \right)^2 \right) \right]. \end{aligned}$$

for $s = 1, \dots, 4$, where $\sigma_s = (10, 13, 16, 19)$. The periodic condition is imposed on the space domain $[-1, 1]$ and velocity domain is truncated by $[-15, 15]$. We compute numerical solutions using a time step determined by CFL= 2 up to $t_f = 0.2$. Here we use $N_v = 60$ and $N_x = 40, 80, 160, 320$. For each scheme, we expect to observe both the order of time integration and that of spatial reconstruction.

In Table 1, we report the numerical errors and convergence rates for global number density based on the relative L^1 -norm. Here we confirm that RK2, BDF2 and BDF3 based schemes attain desired accuracies. However, we observe the order reduction with the RK3 based scheme in the limit $\varepsilon \rightarrow 0$, which commonly happens in the stiff problem when we adopt RK methods of order greater than two.

6.2. Indifferentiability principle. The aim of this section is to check if the scheme maintains the indifferentiability principle of (2.7). For this, we show a mixture of four equal gases behaves like a single gas, independently of ε . In this test, we assume $\kappa = \varepsilon$.

6.2.1. Single gas and a mixture of four gases. We start from the comparison of single gas and a mixture of four gases. Here we consider following numerical setting:

- (1) Single gas ($L = 1$): Consider a single monoatomic gas of molecular mass $m_1 = 58.5$ with collision frequency $\lambda_{11} = 5$. We take the Maxwellian as initial data which

	$N_x, 2N_x$	$\varepsilon = 10^{-5}$		$\varepsilon = 10^{-4}$		$\varepsilon = 10^{-3}$		$\varepsilon = 10^{-2}$	
		error	rate	error	rate	error	rate	error	rate
RK2 QW23	40, 80	3.01e-03	1.97	2.95e-03	2.03	2.50e-03	2.35	8.88e-04	2.72
	80, 160	7.69e-04	2.07	7.22e-04	2.15	4.90e-04	2.65	1.35e-04	2.93
	160, 320	1.84e-04		1.63e-04		7.81e-05		1.78e-05	
BDF2 QW23	40, 80	3.58e-03	1.97	3.54e-03	2.01	3.04e-03	2.28	1.15e-03	2.59
	80, 160	9.14e-04	1.83	8.76e-04	1.88	6.27e-04	2.48	1.91e-04	2.76
	160, 320	2.57e-04		2.38e-04		1.13e-04		2.82e-05	
RK3 QW35	40, 80	2.46e-03	1.97	2.33e-03	2.19	1.69e-03	2.93	1.00e-03	4.23
	80, 160	6.30e-04	1.88	5.09e-04	2.89	2.22e-04	4.39	5.35e-05	4.73
	160, 320	1.71e-04		6.85e-05		1.06e-05		2.02e-06	
BDF3 QW35	40, 80	2.74e-03	2.01	2.65e-03	2.06	2.16e-03	2.81	7.86e-04	4.49
	80, 160	6.79e-04	3.43	6.37e-04	3.02	3.08e-04	3.58	3.51e-05	4.92
	160, 320	6.28e-05		7.86e-05		2.58e-05		1.16e-06	

TABLE 1. Accuracy test for SL methods associated to initial data (6.2).

reproduce

$$(6.3) \quad \begin{aligned} n_0(x) &= \frac{4}{m_1}, \quad T_0(x) = \frac{4}{n_0^1}, \\ u_0(x) &= \frac{1}{10} \left[\exp \left(- \left(10x - 1 + \frac{1}{3} \right)^2 \right) - 2 \exp \left(- \left(10x + 3 - \frac{1}{10} \right)^2 \right) \right]. \end{aligned}$$

- (2) Four gases ($L = 4$): For fair comparison with the single gas case, we consider a mixture of binary gases whose molecular masses are given by

$$m_1 = m_2 = m_3 = m_4 = 58.5,$$

with $\lambda_{sk} = 5$ for all $1 \leq s, k \leq L$. We also set initial data by the Maxwellian whose macroscopic fields are given as follows:

$$(6.4) \quad \begin{aligned} n_0^s(x) &= \frac{1}{m_1}, \quad T_0^s(x) = \frac{4}{\sum_{s=1}^4 n_0^s}, \\ u_0^s(x) &= \frac{1}{10} \left[\exp \left(- \left(10x - 1 + \frac{1}{3} \right)^2 \right) - 2 \exp \left(- \left(10x + 3 - \frac{1}{10} \right)^2 \right) \right]. \end{aligned}$$

for $s = 1, 2, 3, 4$.

For both cases, We impose the periodic boundary condition on the space domain $[-1, 1]$ and truncate velocity domain by $[-15, 15]$. We compute numerical solutions with $N_v = 60$, $N_x = 200$ up to a final time $t_f = 0.2$. For a time interval $t \in (0, 0.02]$, due to the use of not well-prepared initial data we set CFL=0.2. After then we continue the computation with CFL=2.

In Tab. 2, we report the discrepancy of solutions of single gas and four gases using the relative L^1 -norm. For various ranges of $\varepsilon = 10^{-q}$, $q = 2, 3, 4, 5$, we observe that the spatial errors are dominant with respect to time errors and the accuracy of BDF3-QCW35 scheme is confirmed. In Fig. 2, we note that both solutions show good agreements to each other for $q = 2$. Similar results are obtained with the other schemes proposed in the paper.

	N_x	$\varepsilon = 10^{-5}$		$\varepsilon = 10^{-4}$		$\varepsilon = 10^{-3}$		$\varepsilon = 10^{-2}$	
		error	rate	error	rate	error	rate	error	rate
n	100	4.73e-06	3.26	4.22e-06	3.30	1.93e-06	3.44	4.37e-07	3.80
	200	4.95e-07	4.17	4.28e-07	4.33	1.78e-07	4.60	3.15e-08	4.86
	400	2.76e-08		2.12e-08		7.36e-09		1.09e-09	
u	100	2.68e-04	3.39	2.44e-04	3.47	1.17e-04	3.67	3.23e-05	4.01
	200	2.55e-05	4.11	2.21e-05	4.28	9.20e-06	4.65	2.01e-06	4.94
	400	1.48e-06		1.14e-06		3.66e-07		6.55e-08	
T	100	3.16e-06	3.31	2.83e-06	3.38	1.34e-06	3.55	2.92e-07	3.72
	200	3.19e-07	4.21	2.71e-07	4.37	1.14e-07	4.61	2.21e-08	4.92
	400	1.72e-08		1.31e-08		4.70e-09		7.28e-10	

TABLE 2. BDF3-QCW35. The discrepancy of solutions for 4gas and 1gas. Numerical solutions are computed with initial data (6.3) and (6.4).

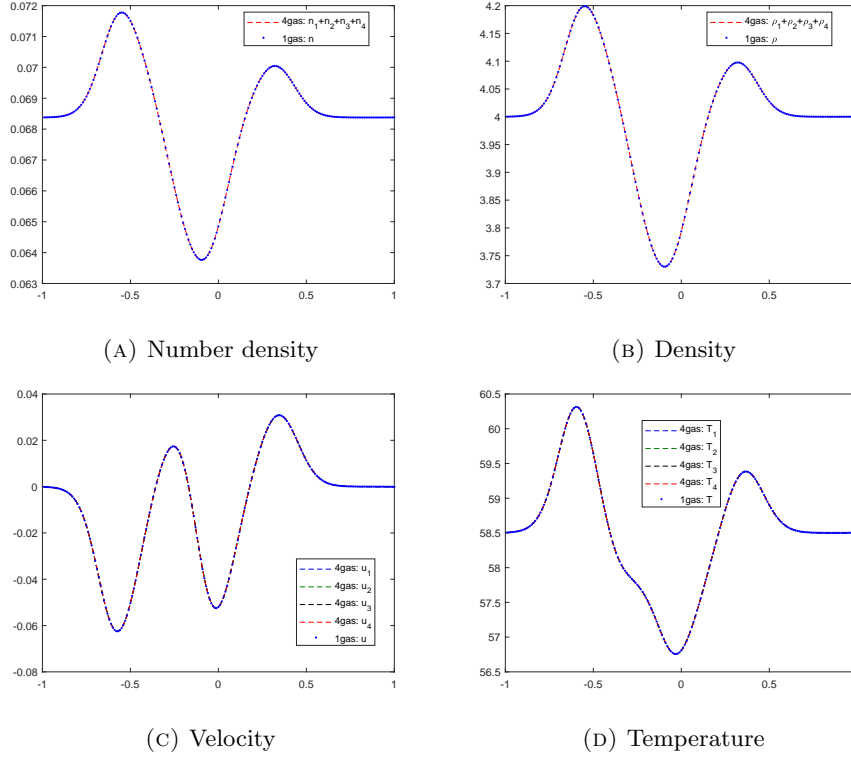


FIGURE 2. BDF3-QCWENO35 for $\varepsilon = 10^{-2}$ associated to initial data (6.3) and (6.4).

6.3. Comparison with classical Euler system (2.16). In this test, we aim to check if the proposed scheme gives correct solutions in the Euler limit. For this, we consider a test in [18]. The molecular masses and value of λ_{sk} follows the choice in (6.1). The Maxwellian

is taken as initial data, which reproduces the following macroscopic fields:

$$(\rho_0, u_0, p_0) = \begin{cases} (1, 0, 5/3), & x < 0.5 \\ (1/8, 0, 1/6), & x > 0.5, \end{cases}$$

$$(\rho_{01}, \rho_{02}, \rho_{03}, \rho_{04}) = \begin{cases} (1/10, 2/10, 3/10, 4/10), & x < 0.5 \\ (1/80, 2/80, 3/80, 4/80), & x > 0.5. \end{cases}$$

We assume the freeflow boundary condition on the spatial domain $[-1, 1]$ and truncate velocity domain by $[-15, 15]$. We compute numerical solutions with $N_x = 200$ and $N_v = 60$ upto $T_f = 0.2$. As in the previous test, we set CFL=0.2 for $t \in (0, 0.2]$ and CFL=2 for $t \in (0.2, 2]$ for this test. We take $\varepsilon = \kappa = 10^{-6}$

In Figure 3, we compare our solution with the reference solution obtained by solving the classical Euler system (2.16) with explicit RK3 method and WENO23 (with 4000 grid points). The numerical solutions show good agreement with the reference solutions. In particular, we can observe that each species velocity and temperature recovers the same global velocity and temperature of gas mixture. This result also verifies that the proposed scheme has the asymptotic preserving property.

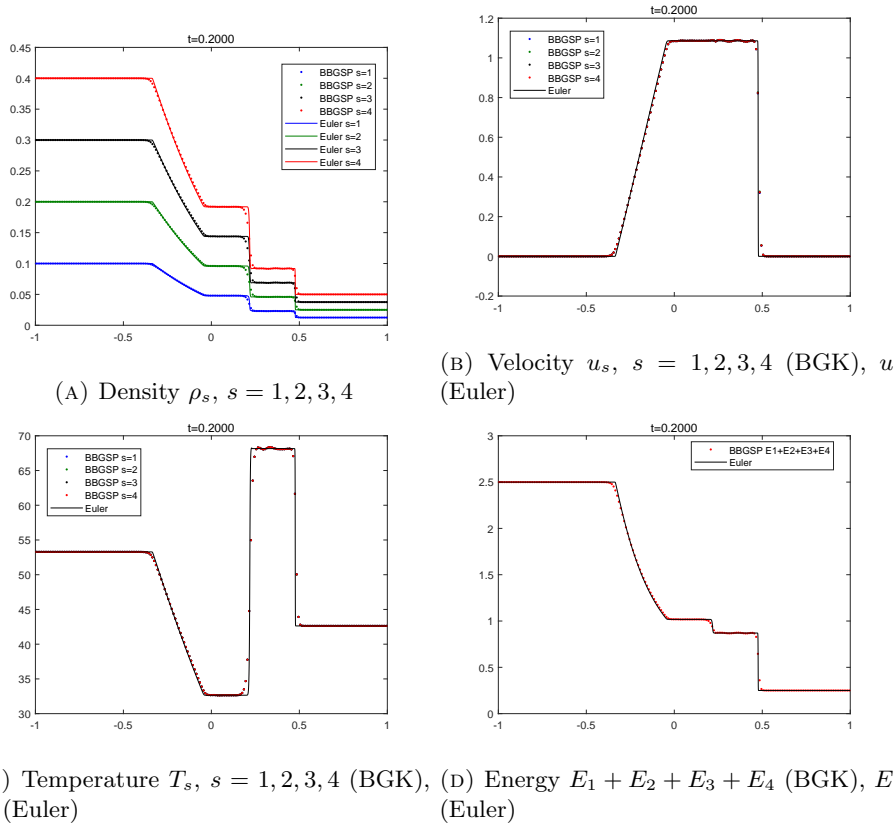


FIGURE 3. BDF3-QCW35 for $\varepsilon = 10^{-6}$ associated to initial data in section 6.3. Reference solutions are plotted by black line '—'.

6.4. Comparison with multi velocities and temperatures Euler system (2.17). In the limit $\kappa \rightarrow 0$, we expect the solution to (2.17) converges to that of (2.16). To confirm this asymptotic behavior, we consider the same numerical setting in section 6.3. We set a small fixed value of $\varepsilon = 10^{-6}$, and take different values of $\kappa = 10^{-q}$, $q = 1, 2, 3, 4$.

In Figures 4-5, we compare our solutions (dotted lines) with the reference solution (solid lines) to (2.17) obtained by explicit RK3 method with WENO23 with 4000 grid points.

We first consider two extreme cases: $\kappa = 10^{-1}$ (left column of Fig. 4) and $\kappa = 10^{-6}$ (Fig. 3). For $\kappa = 10^{-1}$, there are few collisions between gas molecules of different species, and the behavior of each gas is almost independent from the other gases. On the contrary, when there are more frequent collisions $\kappa = 10^{-6}$ (right column of Fig. 3) each species velocity and temperature converges to the same one. This is what we expect to show with two different Euler models (2.16) and (2.17). Also, in the intermediate regime, say $\kappa = 10^{-3}$, (left column of Fig. 5) there is an interesting observation about the species velocity and temperature profiles. Gas particles travel from right to left. Light particles are affected by the shock earlier than heavy particles, and in the interaction they tend to change their velocity more quickly. This explains why the change in the energy appears first in the light particles than in the heavy particles. Also, the light particles change their velocities much quicker than the heavy particles, and this is why there is a peak in the kinetic energy, illustrated by the overshoot in the green velocity profile; on the contrary, the effect of the collision on the heavy particles is slightly delayed, and it first manifests with the increase of their temperature, similar to the Brownian motion effect, which explains the blue peak in the temperature profile. All such effects appear on a much shorter time scale for a smaller value of the parameter κ , as illustrated in Fig. 5. From the matches of the numerical solutions and reference solutions for various range of κ , we verified that our SL scheme is able to capture the correct limit to the multi velocities and temperatures Euler system (2.17). We can also confirm that the behavior of the single velocity and temperature Euler system (2.16) can be described by the multi velocities and temperatures Euler system (2.17) in the limit $\kappa \rightarrow 0$. Consequently, we can say that our scheme is asymptotic preserving.

CONCLUSION

This papers presents high order conservative semi-Lagrangian schemes applied to a recent consistent BGK model for inert mixtures [7]. Thanks to its structure, this BGK model allows different asymptotic limits in collision dominated regimes, depending on if all collisions are equally dominant or if only the intra-species ones are the leading process in the evolution of the mixture. Correspondingly, at zero order asymptotic with respect to a small Knudsen number ε , Euler equations involving global velocity and temperature or species velocities and temperatures can be derived. High order conservative semi-Lagrangian schemes presented here are unconditionally stable, and hence it enables to reproduce the correct behavior of Euler equations without resorting to CFL-type time step restriction. The accuracy of the methods and their convergence rates are tested on a sample case. Then, the indifferenciability principle, which can be proved analytically, is shown to be fulfilled numerically at the desired accuracy. Finally, the AP property is numerically demonstrate on a Riemann problem considering first the classical Euler equations, when all collisions are dominant, and then versus the multi-velocity and temperature Euler system. In this last case, we have shown the trends towards the classical limit, when the parameter κ becomes of the same order of *epsilon*. It has been observed the opposite behaviours in the variation of species velocities and temperature of light and heavy gases, in case of disparate masses. Realistic

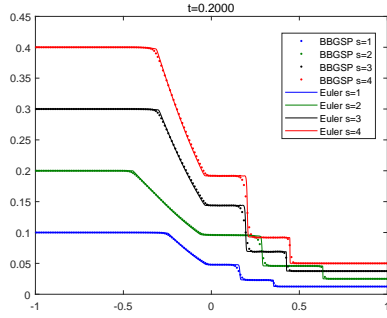
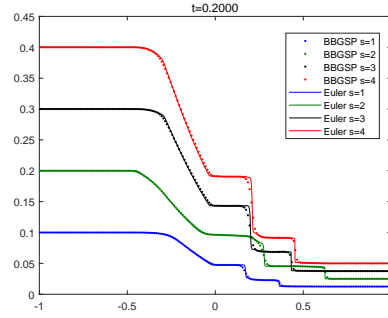
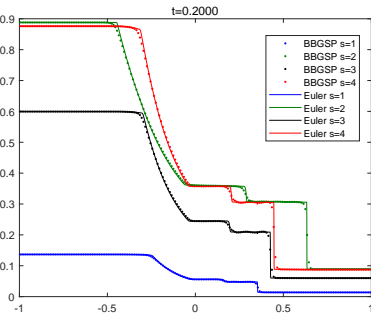
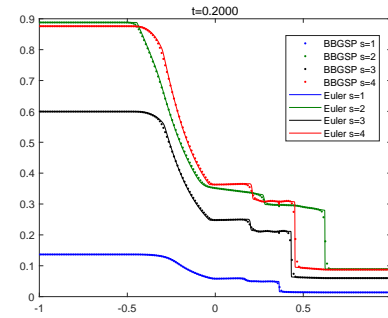
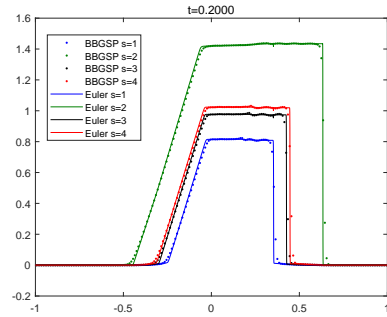
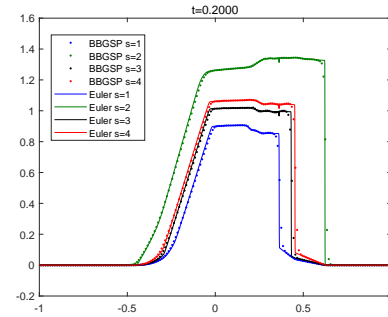
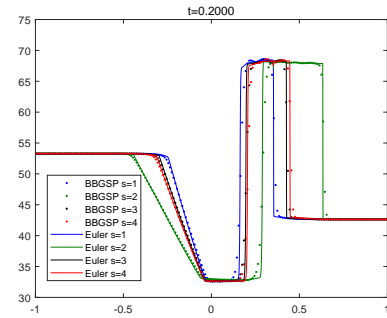
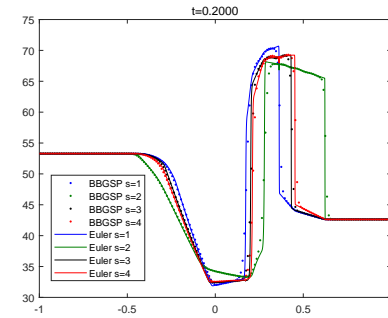
(A) Density ρ_s , $s = 1, 2, 3, 4$ (B) Density ρ_s , $s = 1, 2, 3, 4$ (C) Energy E_s , $s = 1, 2, 3, 4$ (D) Energy E_s , $s = 1, 2, 3, 4$ (E) Velocity u_s , $s = 1, 2, 3, 4$ (F) Velocity u_s , $s = 1, 2, 3, 4$ (G) Temperature T_s , $s = 1, 2, 3, 4$ (H) Temperature T_s , $s = 1, 2, 3, 4$

FIGURE 4. BDF3-QCW35 for $(\varepsilon, \kappa) = (10^{-6}, 10^{-1})$ (left) and $(\varepsilon, \kappa) = (10^{-6}, 10^{-2})$ (right) associated to initial data in section 6.4.

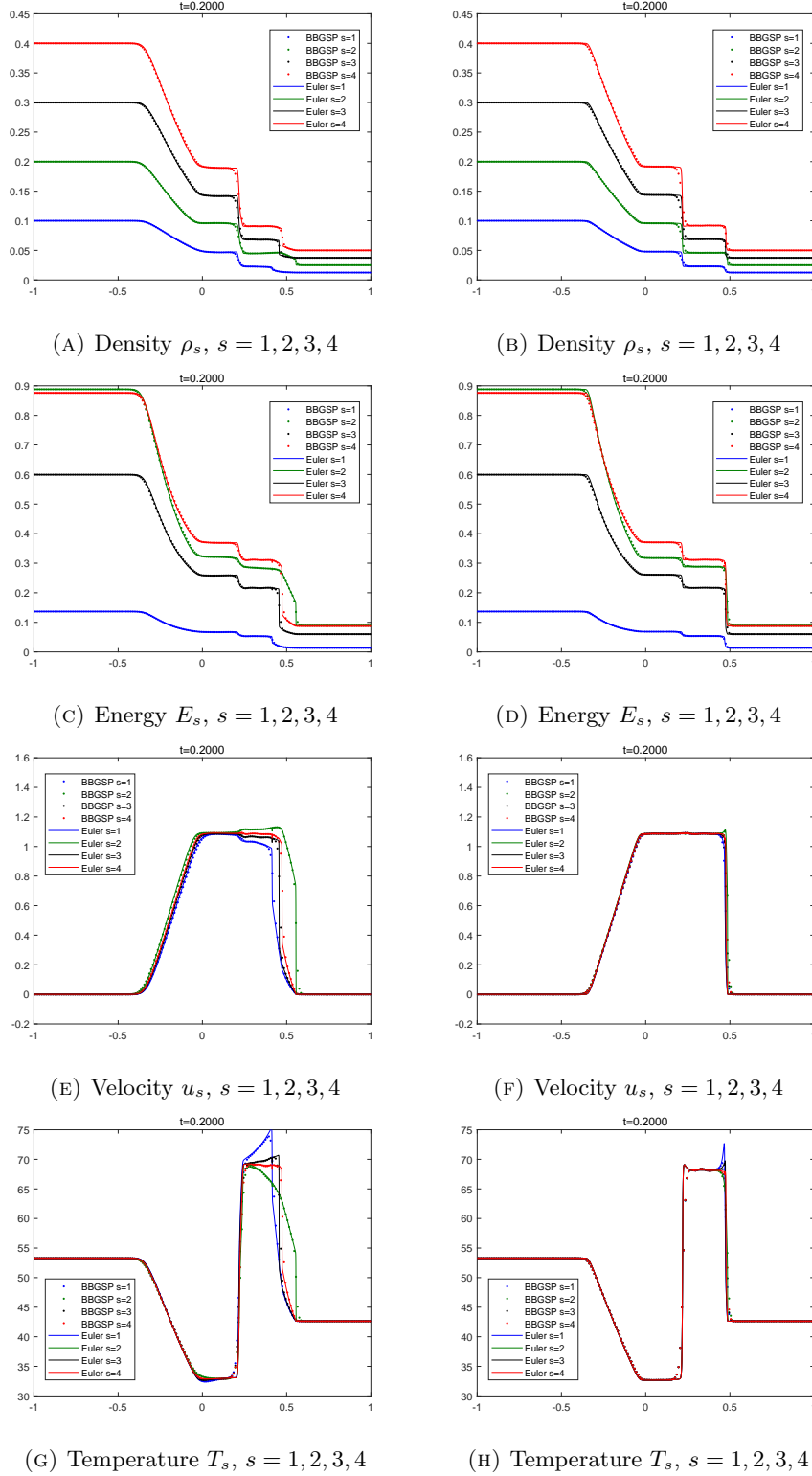


FIGURE 5. BDF3-QCW35 for $(\varepsilon, \kappa) = (10^{-6}, 10^{-3})$ (left) and $(\varepsilon, \kappa) = (10^{-6}, 10^{-4})$ (right) associated to initial data in section 6.4.

applications to noble gases, as well as comparisons at Navier Stokes levels, will be discussed in a forthcoming paper [11].

ACKNOWLEDGEMENT

S. Y. Cho has been supported by ITN-ETN Horizon 2020 Project ModCompShock, Modeling and Computation on Shocks and Interfaces, Project Reference 642768. S. Y. Cho, S. Boscarino and G. Russo would like to thank the Italian Ministry of Instruction, University and Research (MIUR) to support this research with funds coming from PRIN Project 2017 (No. 2017KKJP4X entitled “Innovative numerical methods for evolutionary partial differential equations and applications”). S. Boscarino has been supported by the University of Catania (“Piano della Ricerca 2016/2018, Linea di intervento 2”). S. Boscarino and G. Russo are members of the INdAM Research group GNCS. M. Groppi thanks the support by the University of Parma, by the Italian National Group of Mathematical Physics (GNFM-INdAM), and by the Italian National Research Project “Multiscale phenomena in Continuum Mechanics: singular limits, off-equilibrium and transitions” (PRIN 2017YBKNCE).

REFERENCES

- [1] A. Aimi, M. Diligenti, M. Groppi, C. Guardasoni, *On the numerical solution of a BGK-type model for chemical reactions*, Eur. J. Mech. B Fluids, 26(4):455–472, 2007.
- [2] P. Andries, K. Aoki, B. Perthame, *A consistent BGK-type model for gas mixtures*, J. Stat. Phys., 106(5-6):993–1018, 2002.
- [3] P. L. Bhatnagar, E. P. Gross and K. Krook, *A model for collision processes in gases*, Phys. Rev. 94:511–524, 1954.
- [4] M. Bisi, A. V. Bobylev, M. Groppi, G. Spiga, *Hydrodynamic equations from a BGK model for inert gas mixtures*, In AIP Conference Proceedings, 2132(1):130010, AIP Publishing LLC, 2019.
- [5] M. Bisi, M. Groppi, G. Martalò, *Macroscopic equations for inert gas mixtures in different hydrodynamic regimes*, J. Phys. A: Math. and Theor., in press, DOI: 10.1088/1751-8121/abbd1b, 2020.
- [6] M. Bisi and M. J. Caceres, *A BGK relaxation model for polyatomic gas mixtures*, Commun. Math. Sci. 14(2):297–325, 2016.
- [7] Bobylev, A. V., Bisi, M., Groppi, M., Spiga, G. Potapenko, I. F., *A general consistent BGK model for gas mixtures*, Kinet. Relat. Models, 11(6):1377, 2018.
- [8] S. Boscarino, S.-Y. Cho, G. Russo and S.-B. Yun, *High order conservative Semi-Lagrangian scheme for the BGK model of the Boltzmann equation*, Commun. Comput. Phys., 29(1): 1–56, 2021.
- [9] S. Boscarino, S. Y. Cho, G. Russo, S.-B. Yun, *Convergence estimates of a semi-Lagrangian scheme for the ellipsoidal BGK model for polyatomic molecules*, arXiv preprint arXiv:2003.00215, submitted, 2020.
- [10] C. Cercignani, *Theory and application of the Boltzmann equation*. Scottish Academic Press, 1975.
- [11] S. Y. Cho, S. Boscarino, M. Groppi, G. Russo, *BGK models for inert mixtures and their hydrodynamic limits: comparison and applications*, in preparation.
- [12] S. Y. Cho, S. Boscarino, G. Russo, S.-B. Yun, *Conservative semi-Lagrangian schemes for kinetic equations Part I: Reconstruction*, arXiv preprint arXiv:2007.13167, submitted, 2020.
- [13] S. Y. Cho, S. Boscarino, G. Russo, S.-B. Yun, *Conservative semi-Lagrangian schemes for kinetic equations Part II: Applications*, arXiv preprint arXiv:2007.13166, submitted, 2020.
- [14] C. K. Chu, *Kinetic-theoretic description of the formation of a shock wave*, Phys. Fluids, 8(1):12–22, 1965.
- [15] I. Cravero, G. Puppo, M. Semplice and G. Visconti, *CWENO: uniformly accurate reconstructions for balance laws*. Math. Comp. 87:1689–1719, 2018.
- [16] I. M. Gamba and S. H. Tharkabhushaman, *Spectral-Lagrangian based methods applied to computation of non-equilibrium statistical states*, J. Comput. Phys., 228(6):2012–2036, 2009.
- [17] M. Groppi, G. Russo and G. Stracquadanio, *High order semi-Lagrangian methods for the BGK equation*, Commun. Math. Sci. 14(2):389–414, 2016.
- [18] M. Groppi, G. Russo and G. Stracquadanio, *Semi-Lagrangian Approximation of BGK Models for Inert and Reactive Gas Mixtures*, In: “From Particle Systems to Partial Differential Equations V”, Springer Proceedings in Mathematics and Statistics 258, Patricia Gonçalves and Ana Jacinta Soares (Eds.):53–80, 2018.

- [19] M. Groppi and G. Spiga, *A Bhatnagar-Gross-Krook-type approach for chemically reacting gas mixtures*, Phys. Fluids, 16(12): 4273–4284, 2004.
- [20] E. Hairer, G. Warner, *Solving Ordinary Differential Equations II: Stiff and Differential-Algebraic Problems* (Springer Series in Computational Mathematics 14), Springer, Berlin, 1996.
- [21] S. Jin and Z. Xin, *The relaxation schemes for systems of conservation laws in arbitrary space dimensions*, Commun. Pure Appl. Math., 48(3):235–276, 1995.
- [22] D. Levy, G. Puppo, G. Russo, *Central WENO schemes for hyperbolic systems of conservation laws*, ESAIM: Math. Model. Numer. Anal., 33(3): 547–571, 1999.
- [23] D. Madjarević and S. Simić, *Shock structure in helium-argon mixture—a comparison of hyperbolic multi-temperature model with experiment*, EPL, 102(4):44002, 2013.
- [24] L. Mieussens, *Discrete velocity model and implicit scheme for the BGK equation of rarefied gas dynamics*, Math. Models Methods Appl. Sci., 10(08):1121–1149, 2000.
- [25] T. Ruggeri and S. Simić, *On the hyperbolic system of a mixture of Eulerian fluids: a comparison between single- and multi-temperature models*, Math. Methods Appl. Sci., 30(7):827–849, 2007.
- [26] G. Russo and P. Santagati, *A new class of large time step methods for the BGK models of the Boltzmann equation*, arXiv:1103.5247v1, 2011.
- [27] G. Russo and S. B. Yun, *Convergence of a semi-Lagrangian scheme for the ellipsoidal BGK model of the Boltzmann equation*, SIAM J. Numer. Anal., 56(6):3580–3610, 2018.
- [28] S. Simić, M. Pavic-Colic and D. Madjarević, *Non-equilibrium mixtures of gases: modelling and computation*, Riv. di Mat. della Univ. di Parma, 6(1):135–214, 2015.
- [29] P. Welander, *On the temperature jump in a rarefied gas*, Ark. Fys. 7:507–533, 1954.

SEUNG YEON CHO, DEPARTMENT OF MATHEMATICS AND COMPUTER SCIENCE, UNIVERSITY OF CATANIA, 95125 CATANIA, ITALY
Email address: chosy89@skku.edu

SEBASTIANO BOSCARINO, DEPARTMENT OF MATHEMATICS AND COMPUTER SCIENCE, UNIVERSITY OF CATANIA, 95125 CATANIA, ITALY
Email address: boscarino@dmf.unict.it

MARIA GROPPi, DEPARTMENT OF MATHEMATICAL, PHYSICAL AND COMPUTER SCIENCES, UNIVERSITY OF PARMA, PARCO AREA DELLE SCIENZE 53/A, 43124 PARMA, ITALY
Email address: maria.groppi@unipr.it

GIOVANNI RUSSO, DEPARTMENT OF MATHEMATICS AND COMPUTER SCIENCE, UNIVERSITY OF CATANIA, 95125 CATANIA, ITALY
Email address: russo@dmf.unict.it